Journal of Anatomy

J. Anat. (2012) **220**, pp77–85 doi: 10.1111/j.1469-7580.2011.01449.x

Structural and functional changes in the alveolar bone osteoclasts of estrogen-treated rats

Ana Paula de Souza Faloni,[1] Estela Sasso-Cerri,[1,2] Fernanda Regina Godoy Rocha,[2] Eduardo Katchburian[1] and Paulo Sérgio Cerri[1,2]

[1]*Department of Morphology and Genetics, Federal University of São Paulo (UNIFESP), São Paulo, Brazil*
[2]*Laboratory of Histology and Embryology, Dental School, UNESP – Universidade Estadual Paulista, São Paulo, Brazil*

Abstract

This study investigated structural and functional features of apoptotic alveolar bone osteoclasts in estrogen-treated rats. For this purpose, 15 female rats 22 days old were divided into three groups: Estrogen (EG), Sham (SG) and Control (CG). The rats of EG received daily intramuscular injection of estrogen for 7 days. The SG received only the oil vehicle. Maxillary fragments containing alveolar bone were removed and processed for light and transmission electron microscopy. Area (OcA) and number of nuclei (OcN) and bone resorption surface per TRAP-positive osteoclasts (BS/OC) were obtained. Vimentin, caspase-3 and MMP-9 immunoreactions, TUNEL/TRAP and MMP-9/TUNEL combined reactions were performed. In EG, the OcA, OcN and BS/Oc were reduced. Moreover, osteoclasts showed cytoplasm immunolabelled by caspase-3 and a different pattern of vimentin expression in comparison with CG and SG. MMP-9 expression was not affected by estrogen and the TUNEL-positive osteoclasts were MMP-9-immunolabelled. In EG, ultrastructural images showed that apoptotic osteoclasts did not exhibit ruffled borders or clear zones and were shedding mononucleated portions. TRAP-positive structures containing irregular and dense chromatin were partially surrounded by fibroblast-like cells. In conclusion, the reduction in the BS/Oc may be due to reduction in OcA and OcN; these effects seem to be related to vimentin disarrangement rather than to an interference of estrogen with osteoclast MMP-9 expression. Osteoclast apoptosis involves caspase-3 activity and vimentin degradation; these cells release portions containing one apoptotic nucleus and, subsequently, undergo fragmentation, giving rise to apoptotic bodies.
Key words: apoptosis; estradiol; MMP-9; osteoclast; vimentin.

Introduction

Osteoclast formation, activity and survival are under the influence of several systemic, local and environmental factors (Phan et al. 2004). Among the systemic factors, estrogen is a steroid hormone widely known for its inhibitory function on bone resorption (Tapp, 1966; Liu & Howard, 1991; Chow et al. 1992; Faloni et al. 2007; Cruzoé-Souza et al. 2009). The inhibition of bone resorption by estrogen seems to be associated, at least in part, to the inhibition of osteoclast proteases (Parikka et al. 2001). Bone resorption depends on the activity of different enzymes such as tartrate-resistant acid phosphatase (TRAP), cathepsin K and matrix metalloproteinase-9 (MMP-9); these enzymes are osteoclast markers (Sorensen et al. 2007). Among them, the MMP-9, a zinc-dependent proteinase also called gelatinase B, seems to degrade peptides derived from collagenase activity and other components of the bone matrix (Sternlicht & Werb, 2001).

Studies including different models have suggested that estrogen is able to promote osteoclast apoptosis but the mechanism is still unclear (reviewed by Saintier et al. 2006; Faloni et al. 2007; Cruzoé-Souza et al. 2009). The treatment of young female rats with estrogen has caused a 50% reduction in the number of alveolar bone osteoclasts due to osteoclast death by apoptosis (Faloni et al. 2007; Cruzoé-Souza et al. 2009). The presence of enhanced estrogen receptor-beta (ER-β) immunoexpression in the apoptotic osteoclasts suggests that estrogen may act directly on osteoclasts by controlling their survival (Cruzoé-Souza et al. 2009).

In mononuclear cells, programmed cell death by apoptosis involves a complex and coordinated cascade of molecular events. This cascade involves caspases, such as caspase-3, responsible for degradation of the nuclear proteins and activation of nucleases which induce the degradation of

Correspondence
Prof. Dr. Paulo Sérgio Cerri, Laboratory of Histology and Embryology, Department of Morphology, Dental School, UNESP – Univ Estadual Paulista, Rua Humaitá, 1680, Centro, CEP 14801–903, Araraquara, São Paulo, Brazil. T: + 55 16 33016497; F: + 55 16 33016433;
E: pcerri@foar.unesp.br

Accepted for publication *11 October 2011*
Article published online *16 November 2011*

DNA (Huppertz et al. 1999). In addition, it is known that caspase-3 cleaves cytoplasmic proteins of the cytoskeleton, such as vimentin (Byun et al. 2001; Alam et al. 2010). Osteoclasts exhibit vimentin filaments distributed around the nuclei and in the ruffled border region (Akisaka et al. 2008) and, therefore, these filaments have an essential role in osteoclast polarization and maintenance of the structural integrity of osteoclast. Thus, the degradation of cytoskeleton proteins induces its disruption and collapse (Byun et al. 2001; Lee et al. 2002; Alam et al. 2010). Subsequently, the apoptotic cell undergoes blebbing and sheds apoptotic bodies (Huppertz et al. 1999; Cerri et al. 2000; Cerri, 2005).

In young rats, numerous osteoclasts are observed in the alveolar bone surface due to the continuous and intense bone remodelling to accommodate the growing and eruption tooth. As apoptosis is a rapid process, the effect of estrogen in alveolar bone of young animals is a suitable *in vivo* model to investigate the apoptotic process in osteoclasts (Faloni et al. 2007; Cruzoé-Souza et al. 2009).

In the present study, we propose to investigate the estrogen effect on the structural and functional integrity of osteoclasts. As the number of nuclei and area of osteoclasts are indicative parameters of resorptive activity (Chow et al. 1992; Lees & Heersche, 2000; Lees et al. 2001), we examined these parameters and related them to the bone resorption surface. A possible relationship between apoptotic process and vimentin/MMP-9 immunoexpression was also examined in the alveolar bone osteoclasts.

Materials and methods

Animals and treatment

The animal care laws and national laws on animal use were observed in this study, which was authorized by the Ethical Committee for Animal Research of the Federal University of São Paulo (UNIFESP), Brazil.

Fifteen female Holtzman rats (*Rattus norvegicus albinus*) 22 days old were equally distributed into Estrogen (EG), Sham (SG) and Control (CG) Groups. For 7 days, rats from the EG received a daily intramuscular injection of 0.125 mg 100 g^{-1} body weight of estrogen (estradiol hexahydrobenzoate, Benzoginoestril ap®; Hoechst Marion Roussel, São Paulo, Brazil) diluted in corn oil. The dosage of estrogen and the period of administration used in this study have been shown to cause significant changes in bone metabolism (Silberberg & Silberberg, 1941; Chow et al. 1992).

The SG rats received the same dose of corn oil and the CG rats did not receive any treatment.

Histological procedures

The animals were killed with chloral hydrate (600 mg kg^{-1}) and fragments of the maxilla containing alveolar bone surrounding the upper molars were removed. The specimens were fixed for 48 h at room temperature in 4% formaldehyde (freshly derived from paraformaldehyde) buffered at pH 7.2 with 0.1 M sodium phosphate. After decalcification for 40 days in 7% ethylenediaminetetracetic acid (EDTA) solution containing 0.5% formaldehyde, buffered at pH 7.2 with 0.1 M sodium phosphate, the specimens were dehydrated in graded concentrations of ethanol and embedded in paraffin.

TRAP method and TUNEL/TRAP combined methods

Sagittal sections 6 μm thick, containing alveolar bone, were submitted to the TRAP method. The TRAP method was used as an osteoclast marker (Minkin, 1982; Cerri et al. 2003, 2010). Deparaffinized sections were incubated in a solution containing naphthol AS-BI (Sigma Chemical Co., St. Louis, MO, USA), *N-N*-dimethylformamide, sodium acetate buffer (pH 5.0), Fast Red Salt TR (Sigma Chemical Co.) and sodium tartrate dihydrate.

For detection of DNA breaks (Gavrieli et al. 1992), the TUNEL method was performed as previously described (Cerri et al. 2000, 2003). Deparaffinized sections adhered to silanized (3-aminopropyltriethoxysilane; Sigma Chemical Co.) slices were treated with proteinase K (Oncor-Protein Digesting Enzyme), subsequently treated with 3% hydrogen peroxide to block endogenous peroxidase, and then immersed in an equilibration buffer. The reaction was followed by incubation in solution containing terminal deoxynucleotidyl transferase (TdT) in a humid chamber. The sections were then immersed in the stop/wash solution, incubated in the antidigoxigenin-peroxidase, treated with 0.06% 3.3-diaminobenzidine tetrahydrochloride (Sigma Chemical Co.) and counterstained with Carazzi's haematoxylin. Combined TUNEL and TRAP methods were performed as previously described in detail by Cerri et al. (2003).

Morphometric analysis

Osteoclast area (OcA), number of osteclast nuclei (OcN) and bone resorption surface per osteoclast (BS/Oc)

The morphometric analyses were performed in three non-serial sections of the alveolar bone around the first molar. The smallest distance between the sections was 60 μm. From these sections, 50 TRAP-positive osteoclasts apposed to alveolar bone surface were selected per animal and their images were captured using an image analysis system attached to a light microscope (Jenaval, Zeiss, Germany) at ×1000. To estimate bone resorption activity, the area of osteoclasts (OcA) and the length of the bone surface in close proximity to the zone of contact of each osteoclast (BS/Oc) were measured using the free software IMAGE TOOL (IMAGE TOOL for Windows – Version 3.0; The University of Texas Health Science Center in San Antonio). The number of nuclei (OcN) of each TRAP-positive cell apposed to bone surface was counted.

The data obtained from the morphometric parameters evaluated were distributed in categories. Thus, according to area, the osteoclasts were classified into three categories: small (20.00–199.99 μm^2), medium (200.00–799.99 μm^2) and large (800.00–1746.00 μm^2). On the basis of the number of nuclei/cell, the TRAP-positive cells were classified into mononucleated cells (one nucleus per cellular profile) or multinucleated osteoclasts (two or more nuclei per cellular profile). The length of the bone resorption surface (BS/Oc) was classified into: small (3.03–22.99 μm), medium (23.00–70.99 μm) and large (71.00–118.00 μm).

The frequencies of the different categories of data were obtained for each animal/group and analyzed statistically.

Immunohistochemistry for caspase-3, vimentin and MMP-9 detection

Deparaffinized sections adhered to silanized slides were submitted to immunohistochemistry for caspase-3, vimentin or MMP-9.

Caspase-3

To unmask the antigenic sites, the sections were incubated with 0.1% Triton-X (Aldrich-Chemie, Steinheim, Germany) for 4 h. The sections were incubated overnight with rabbit anti-caspase-3 active form (Millipore Corporation, Temecula, CA, USA) diluted in 1 : 100 phosphate buffer 0.05 M with 0.2 M sodium chloride (phosphate-buffered saline, PBS), pH 7.2. The reaction was detected by Vectastain Kit (Vector Laboratories Inc., Burlingame, CA, USA). Thus, these sections were incubated with biotinylated anti-rabbit/mouse IgG at room temperature and, after washings in PBS, they were incubated with avidin-biotin-peroxidase complex.

Vimentin

To unmask the antigenic sites, the sections were immersed in 0.001 M sodium citrate buffer, pH 6.0, and submitted to microwave oven cycles for 30 min (Sasso-Cerri et al. 2005). The sections were incubated overnight with mouse anti-vimentin (V9, Sigma-Aldrich Inc., St. Louis, MO, USA) diluted in 1 : 150 PBS, in a humidified chamber at 4 °C. After washings in PBS, the vimentin immunoreaction was detected using the MACH 4 Universal HRP-Polymer kit (Biocare Medical LLC., Concord, CA, USA). Thus, the sections were incubated with the MACH 4 mouse probe at room temperature for 15 min, washed in PBS and incubated with MACH 4 HRP polymer at room temperature for 15 min.

MMP-9

Immunohistochemical detection of MMP-9 was performed as previously described (Cerri et al. 2010). To unmask the antigenic sites, the sections were also submitted to microwave oven cycles. Sections were incubated overnight with mouse anti-MMP-9 (Calbiochem®; Biochemicals and Immunochemicals, USA), diluted in 1 : 500 PBS, in a humidified chamber at 4 °C. The reaction was detected by Vectastain Kit (Vector Laboratories Inc., Burlingame, CA, USA). In the CG, SG and EG, the frequency of MMP-9 immunolabelled osteoclasts was evaluated in 30 osteoclasts per animal.

The immunoreactions were revealed by 0.06% 3.3-diaminobenzidine tetrahydrochloride (Sigma-Aldrich, Chemie GmbH, Germany) in PBS and the sections were counterstained with Carazzi's haematoxylin. As negative controls, the immunohistochemistry was performed by replacing the incubation step with primary antibodies using an incubation step with non-immune serum.

Combined immunohistochemistry for MMP-9 and TUNEL reaction

In some sections, MMP-9 detection was performed for the immunohistochemistry and, subsequently, the same sections were submitted to the TUNEL method and revealed using a Vip Substrate Kit (Vector Laboratories Inc.). After washings in distilled water, the sections were counterstained with methyl green (Cruzoé-Souza et al. 2009).

The sections submitted to the TRAP method and TUNEL/TRAP combined methods and sections submitted to immunohistochemistry for caspase-3, vimentin, MMP-9 detection and MMP-9/TUNEL combined reactions were analyzed and the images were captured using an Olympus BX-51 light microscope.

Statistical analysis

The parametric one-way analysis of variance (one-way ANOVA) and the non-parametric Kruskal–Wallis test followed, respectively, by Tukey and Dunn's multiple comparison tests were used for the statistical analysis. All calculations were performed with the software GRAPH PAD PRISMA 4. The significance level accepted was $P < 0.05$.

Transmission electron microscopy

Specimens containing alveolar bone of the first molar were fixed in a mixture of 4% of glutaraldehyde and formaldehyde (derived from paraformaldehyde) buffered at pH 7.2 with 0.1 M sodium cacodylate, at room temperature. After decalcification in a 7% solution of EDTA containing 0.5% formaldehyde in 0.1 M sodium cacodylate buffer, at pH 7.2, the specimens were washed in 0.1 M sodium cacodylate, pH 7.2. They were then transferred to 0.1 M sodium cacodylate-buffered 1% osmium tetroxide solution for 1 h, at room temperature. Subsequently, the specimens were washed in distilled water and treated with aqueous 2% uranyl acetate for 2 h. The specimens were dehydrated in graded concentrations of ethanol, treated with propylene oxide and then embedded in Araldite. Ultrathin semi-serial sections were collected on formvar-coated single slot grids, stained in alcoholic 1% uranyl acetate and lead citrate solution and examined in a Philips CM 200 transmission electron microscope.

Results

On the alveolar bone surface of the first upper molar of 29-day-old rats from the control (CG) and sham (SG) groups, several giant multinucleated TRAP-positive osteoclasts (Oc) were observed (Fig. 1A). In contrast, few TRAP-positive osteoclasts were found in the alveolar bone surfaces of the estrogen-treated rats (EG). Moreover, in EG (Figs 1B,C), the area and number of nuclei of osteoclasts were apparently reduced in comparison with the control groups (Fig. 1A). Sometimes, mononucleated TRAP-positive structures, exhibiting dense chromatin strongly stained by haematoxylin, were observed in close juxtaposition to osteoclasts in the bone surface of estrogen-treated rats (Fig. 1D). Occasionally, these TRAP-positive structures containing irregular masses of dense chromatin were partially surrounded by fibroblasts-like cells of periodontal ligament (Fig. 1E).

The TUNEL/TRAP combined reactions revealed that some of these mononucleated TRAP-positive structures exhibited TUNEL-positivity (Fig. 1F). In EG, some osteoclasts located next to the bone surface showed shrunken cytoplasm

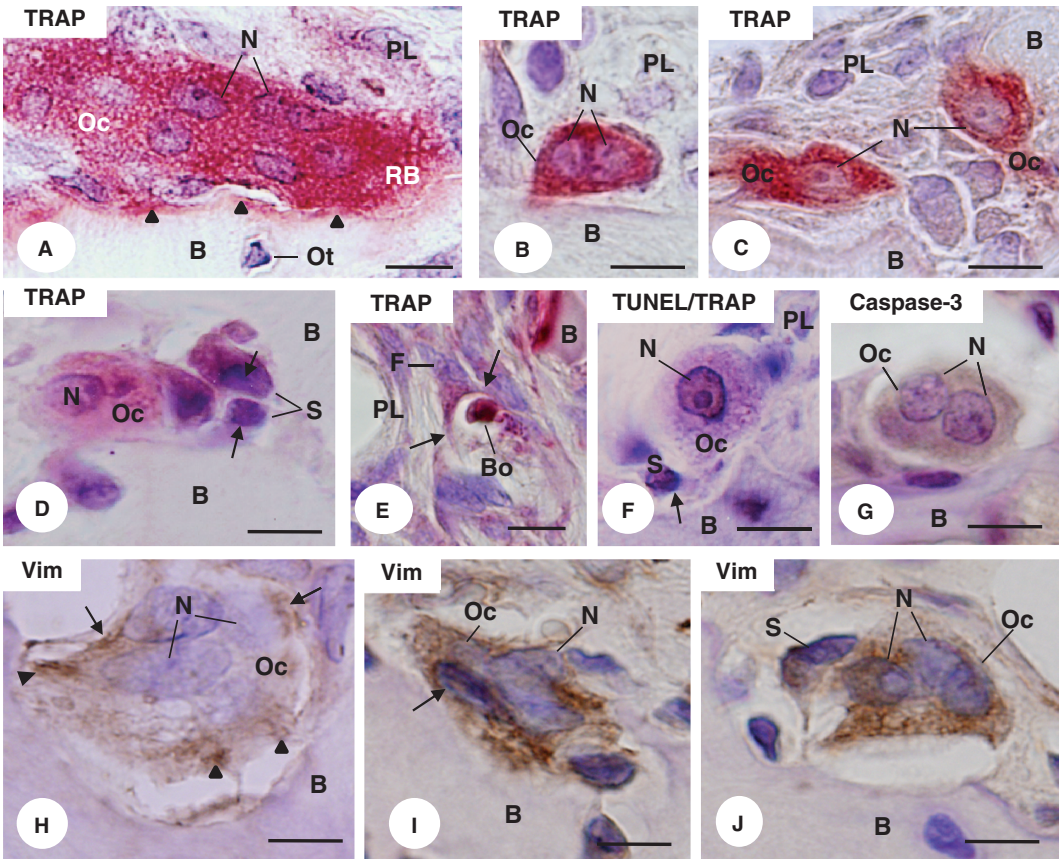

Fig. 1 Light micrographs of portions of alveolar bone (B) from control (A,H) and estrogen-treated (B–G,I ,J) rats. (A–D) TRAP reaction counterstained with haematoxylin. (A) A large TRAP-positive (red colour) osteoclast (Oc) exhibiting several nuclei (N) and ruffled border (RB) is apposed on the bone surface (arrowheads). Osteocyte (Ot). Periodontal ligament (PL). Bar: 5 μm. (B,C) Profiles of TRAP-positive cells (Oc) apposed to the bone surface (B) exhibit only two nuclei (N) and one nucleus (N), respectively. Periodontal ligament (PL). Bar: 5 μm. (D) Adjacent to the alveolar bone surface (B), small TRAP-positive structures (S), which exhibit condensed chromatin strongly stained by haematoxylin (arrows), are in close juxtaposition to a TRAP-positive osteoclast (Oc). Nucleus (N); Bar: 5 μm. (E) A fibroblast-like cell (F) next to the alveolar bone surface (B) engulfs (arrows) a TRAP-positive body (Bo). Periodontal ligament (PL). Bar: 10 μm. (F) Next to the bone surface (B), a mononucleated TRAP-positive cell (Oc) exhibits a TUNEL-positive nucleus (N). In close contact with the TRAP-positive cell (Oc), a structure (S) exhibits an irregular and basophilic body (arrow). Periodontal ligament (PL). TUNEL/TRAP combined methods. Bar: 5 μm. (G) Osteoclast (Oc) in contact with the bone surface (B) shows shrunken cytoplasm immunolabelled by caspase-3 (brown-yellow colour). Nuclei (N). Immunohistochemistry for caspase-3 detection counterstained with haematoxylin. (H–J) Sections of portion of alveolar bone submitted to immunohistochemistry for vimentin detection and counterstained with haematoxylin. (H) Multinucleated osteoclast (Oc) located in an excavation of the bone (B) surface exhibits immunostained cytoplasm for vimentin (brown-yellow colour), mainly around the nuclei (N) (arrows) and in ruffled border area (arrowheads). Bar: 5 μm. (I, J) Osteoclasts (Oc) showing nuclei (N) strongly stained by haematoxylin and apparently shrunken cytoplasm immunolabelled by vimentin (brown-yellow colour); note that the vimentin positivity is spread throughout the cytoplasm. Bar: 5 μm. (I) A mononucleated vimentin-positive structure (S) is in close juxtaposition to the osteoclast (Oc). Bone (B). Bar: 5 μm.

immunolabelled by caspase-3 (Fig. 1G). In CG, multinucleated osteoclasts located in excavations of the bone surface exhibited vimentin-positive cytoplasm, mainly around the nuclei and in the ruffled border area (Fig. 1H). In EG, osteoclasts with condensed chromatin showed vimentin immunoreaction spread throughout the cytoplasm (Fig. 1I–J).

In comparison with CG and SG, the morphometric analyses revealed significant reduction in the OcA, OcN and BS/Oc in EG. No differences were found between CG and SG (Table 1).

The frequency distribution of OcA revealed a significant increase of small osteoclasts in EG in comparison with control groups (CG and SG). Otherwise, large osteoclasts ($\geq$ 800.00 μm^2) were only found in CG and SG (Fig. 2A).

In EG, 48.7% of the total number of TRAP-positive cells exhibited only one nucleus (Fig. 2B). Moreover, the frequency of multinucleated osteoclasts in CG and SG was significantly higher than in EG. It should be noted that osteoclasts with more than six nuclei were found only in CG and SG.

The analysis of the length of bone resorption surface (BS/OC) revealed that BS/Oc varied from 3.0 to 118.0 μm in CG and SG, and from 3.0 to 71.0 μm in EG. Moreover, the frequency of small BS/Oc in EG was significantly higher

Table 1 Mean ± SD of area of osteoclast (OcA), number of nuclei (OcN) and the length of the resorption bone surface per osteoclast (BS/Oc) in the Control (CG), Sham (SG) and Estrogen (EG) Groups.

Groups	OcA (μm^2)	OcN	BS/Oc (μm)
CG	317 ± 43	2.7 ± 0.3	30 ± 2.8
SG	289 ± 47	2.7 ± 0.3	29 ± 1.9
EG	186 ± 17[1,2]	2.1 ± 0.1[3]	21 ± 2.0[4]

[1] $P < 0.01$ vs. SG.
[2] $P < 0.001$ vs. CG.
[3] $P < 0.01$ vs. CG and SG.
[4] $P < 0.001$ vs. CG and SG (Tukey's test).

than in CG and SG. In contrast, large BS/Oc were not found in the EG (Fig. 2C).

The immunohistochemistry for MMP-9 detection showed that multinucleated osteoclasts from the SG (Fig. 3A) and EG (Fig. 3B) located in close contact with bone surface exhibited MMP-9-positive cytoplasm. Quantitative analysis of the frequency of immunolabelled osteoclasts revealed that the differences between the groups were not significant (EG: 82.7 ± 12.0%; CG: 86 ± 5.6% and SG: 75.8 ± 6.1%). However, in the EG, multinucleated MMP-9-positive osteoclasts of varied sizes showed some nuclei with peripheral chromatin strongly stained by haematoxylin (Fig. 3C–F). Next to these osteoclasts, some MMP-9-positive structures exhibiting nuclei strongly stained by haematoxylin were observed (Fig. 3F). The MMP-9/TUNEL combined methods revealed MMP-9-immunolabelled osteoclasts with strongly TUNEL-positive nuclei (Fig. 3G).

Under transmission electron microscope, typical osteoclasts in close contact with the bone surface exhibited a ruffled border, numerous mitochondria, as well as vesicles and vacuoles of varied sizes in the cytoplasmic area next to the ruffled border (Fig. 4A). In EG, some osteoclasts exhibited apparently shrunken cytoplasm and tortuous nuclei with conspicuous masses of peripheral chromatin. Usually, ruffled borders and the clear zones were not found in these altered osteoclasts. The analysis of semi-serial sections showed that cytoplasmatic portions seemed to be shed from these altered osteoclasts; sometimes, these osteoclast portions exhibited irregular-shaped nucleus with blocks of condensed chromatin (Fig. 4B,C).

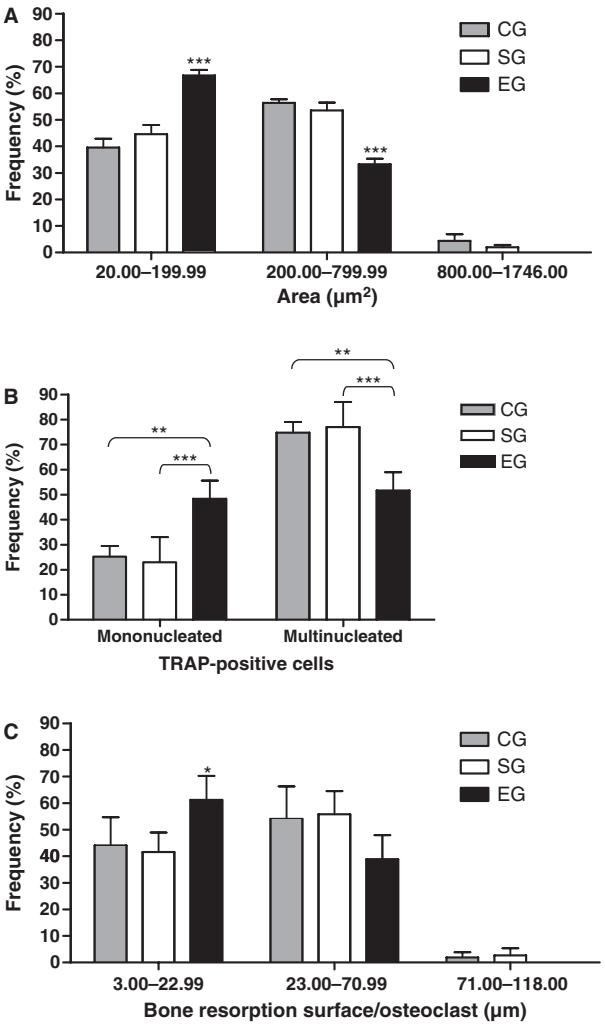

Fig. 2 Frequency (%) of osteoclasts according to area (OcA) (A), number of nuclei (OcN) (B) and bone resorption surface per osteoclast (BS/Oc) (C) in the Control (CG), Sham (SG) and Estrogen (EG) groups. (A) The OcA was classified into: small (20.06–199.99 μm^2), medium (200.00–799.99 μm^2) and large (800.00–1746.00 μm^2). For the first and second categories, $P < 0.05$ (one-way ANOVA). ***$P < 0.001$ vs. CG and SG (Tukey's test). (B) OcN was divided into: mononucleated (one nucleus) and multinucleated (two or more nuclei). For both categories, $P < 0.01$ (one-way ANOVA). ***$P < 0.001$; **$P < 0.01$ vs. CG and SG (Tukey's test). (C) BS/Oc were classified into: small (3.00–22.99 μm), medium (23.00–70.99 μm) and large (71.00–118.00 μm). For the first category, $P < 0.05$ (one-way ANOVA). *$P < 0.05$ vs. CG and SG (Tukey's test).

Discussion

Reduction in the number of alveolar bone osteoclasts in estrogen-treated young female rats has been associated with death of osteoclasts by apoptosis (Faloni et al. 2007; Cruzoé-Souza et al. 2009). Enhanced immunoexpression of estrogen receptors (Erβ) in the apoptotic osteoclasts suggests that estrogen may act directly on osteoclasts by controlling their survival (Cruzoé-Souza et al. 2009). However, the effect of estrogen on the osteoclast structural integrity and activity has not been clarified. In the present study, the images showing TUNEL-positive nuclei in the TRAP-positive osteoclasts in addition to the presence of caspase-3 immunoexpression and the typical apoptotic ultrastructural features, confirmed that estrogen induces apoptosis (Faloni et al. 2007; Cruzoé-Souza et al. 2009). Moreover, the structural integrity of the osteoclasts and the bone resorptive surface were significantly altered, probably due to estrogen-induced cell death by apoptosis.

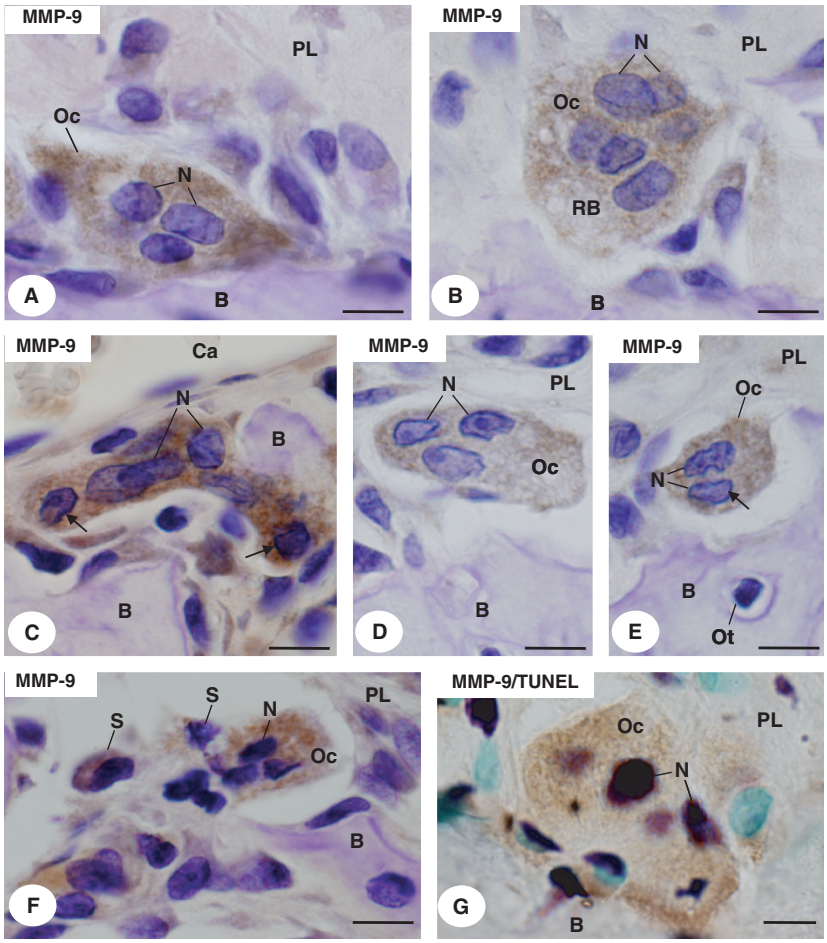

Fig. 3 Light micrographs of portions of alveolar bone (B) of sham (A) and estrogen-treated rats (B–G). (A–F) Portions of alveolar bone (B) submitted to immunohistochemistry for MMP-9 detection (brown-yellow colour) and counterstained with haematoxylin. In (A, B) multinucleated osteoclasts (Oc) located in excavations of the bone surface (B) exhibit MMP-9-positive cytoplasm. Nuclei (N). Ruffled border (RB). Periodontal ligament (PL). (C) A multinucleated osteoclast (Oc), showing MMP-9 immunostaining in the cytoplasm, exhibits two nuclei with peripheral chromatin strongly stained by haematoxylin (arrows). Bone (B). Nuclei (N). Blood capillary (Ca). (D,E) Osteoclasts (Oc) apparently reduced show only three (D) or two (E) nuclei (N); note that a nucleus (arrow) exhibits peripheral condensed chromatin. Osteocyte (Ot). Periodontal ligament (PL). (F) Strongly MMP-9-positive osteoclast (Oc) exhibits nuclei (N) with condensed chromatin. MMP-9-positive structures (S) containing strongly basophilic chromatin are next to the osteoclast (Oc). Periodontal ligament (PL). (G) Portion of alveolar bone (B) submitted to the combined immunohistochemistry for MMP-9 detection (brown-yellow colour) and TUNEL method (purple colour) counterstained with methyl green. A, MMP-9 immunolabelled osteoclast (Oc) shows strongly TUNEL-positive nuclei (N). Periodontal ligament (PL). Bar: 5 μm.

Osteoclast apoptosis involves caspase-3, which has been shown to cleave vimentin, inducing its disruption and collapse of the cytoskeleton in many cell types (Byun et al. 2001; Lee et al. 2002; Saintier et al. 2006; Alam et al. 2010). A cytoskeleton containing vimentin filaments distributed around the nuclei and in the ruffled border region has been described in osteoclasts (Akisaka et al. 2008). In the dying osteoclasts of the estrogen-treated group, the vimentin filaments were distributed throughout the cytoplasm, filling the entire cytosol, as previously shown in dying HeLa cells (Lee et al. 2002). Therefore, the disarrangement of the structural integrity of vimentin filaments in the apoptotic osteoclasts may be due to a possible caspase activation.

When the data regarding the morphometric parameters (OcA, OcN and BS/Oc) were distributed into categories and the frequency of each category was compared among the groups, it was possible to understand better how estrogen affects osteoclast structure and function. In EG, most of the TRAP-positive cells (about 68%) were small osteoclasts; large osteoclasts were not found. Moreover, in the EG, about 50% of these TRAP-positive cells were mononucleated, supporting *in vitro* findings (Saintier et al. 2006). It is not possible to exclude the hypothesis that these mononucleated cells are osteoclast precursors that fail to fuse during osteoclastogenesis, probably due to the estrogen action on the RANK/RANKL/OPG [receptor activator of nuclear factor (NF)-κB/RANK ligand/osteoprotegerin] system (Kawamoto et al. 2002; Rogers et al. 2002; Bord et al. 2003; Kanzaki et al. 2006). However, it is important to note that either the multinucleated osteoclasts or the

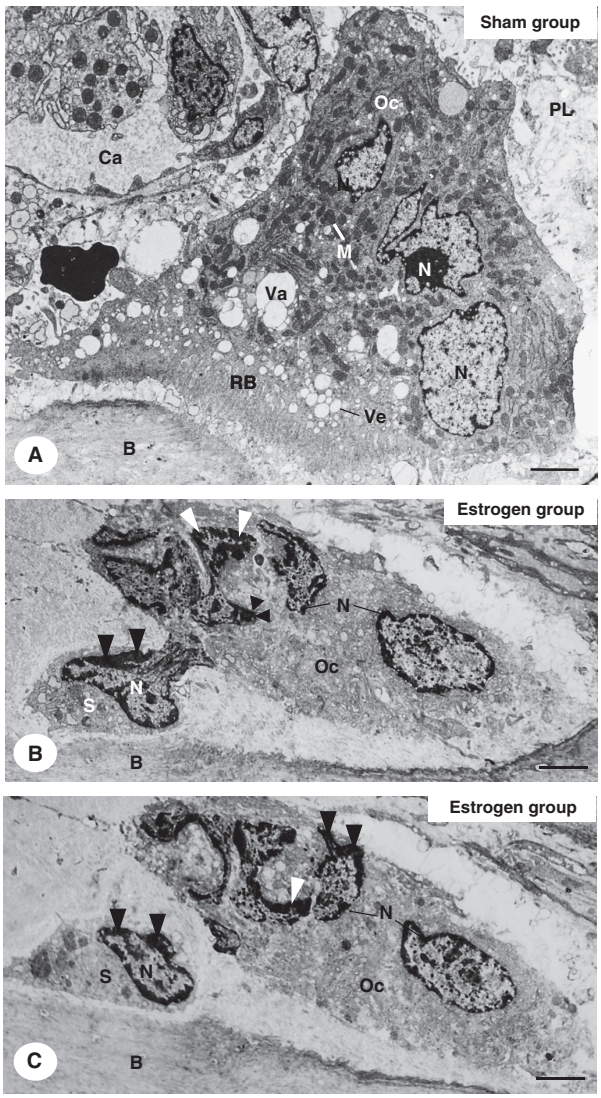

Fig. 4 Electron micrographs of portions of alveolar bone (B) of sham (A) and estrogen-treated (B,C) rats. (A) A typical osteoclast (Oc) is in close contact with the bone surface (B). The osteoclast (Oc) exhibits numerous mitochondria (M), vesicles (Ve) and vacuoles (Va) of varied sizes located next to ruffled border (RB). Nuclei (N). Periodontal ligament (PL). Blood capillary (Ca). Bar: 2 μm. (B,C) Electron micrographs of a portion of alveolar bone (B) of estrogen-treated rat showing semi-serial sections of an osteoclast (Oc). The osteoclast exhibits apparently shrunken cytoplasm and tortuous nuclei (N) with conspicuous masses of peripheral chromatin (arrowheads). The semi-serial sections show that a structure (S) seem to be shedding from the altered osteoclast (Oc); this osteoclast structure (S) exhibits irregular-shaped nucleus (N) with blocks of condensed chromatin (arrowheads). Bar: 2 μm.

mononucleated cells were MMP-9-positive in EG. According to Sorensen et al. (2007), mature or active multinucleated osteoclasts express MMP-9, whereas mononucleated osteoclasts precursors do not. Our results indicate that the mononucleated and/or small osteoclasts (two to three nuclei) observed in EG are derived from the dying osteoclasts by apoptosis. During apoptosis, osteoclasts undergo shrinkage and blebbing, shedding cellular fragments containing TUNEL-positive nuclei. The TUNEL method is used to detect the DNA fragmentation which occurs in apoptosis (Gavrieli et al. 1992; Cerri et al. 2003; Cerri, 2005; Faloni et al. 2007). It is conceivable that the increase in the frequency of medium and of mainly small osteoclasts and the significant increase in the number of mononucleated TRAP-positive cells may be due to shrinkage and fragmentation of osteoclasts during the process of apoptosis. The ultrastructural images confirm that mononucleated cells containing one apoptotic nucleus are probably shed from multinucleated apoptotic osteoclasts. Subsequently, these mononucleated cells undergo fragmentation, probably giving rise to TRAP-positive round and/or ovoid structures containing irregular masses of dense chromatin. These structures, probably apoptotic bodies, were sometimes partially surrounded by cells of periodontal ligament, apparently engulfed by fibroblast-like cells.

The apoptotic features observed in the osteoclasts of estrogen-treated rats are consistent with previous studies under experimental conditions. TUNEL-positive osteoclasts as well as disappearance of ruffled borders and clear zones were also observed in apoptotic osteoclasts of adult rats treated with bisphosphonate (Ito et al. 1999, 2001).

In the present study, the use of pre-pubertal female rats (sexually immature rats) raises the question of whether the morphologic and enzymatic changes in the estrogen-induced apoptotic osteoclasts could be due to a pharmacological/toxic response rather than a physiological response. However, enhanced Erβ immunolabelling was observed in the osteoclasts of pre-pubertal female rats treated with estrogen (Cruzoé-Souza et al. 2009), indicating that exogenous estrogen is able to stimulate the expression of estrogen receptors in these cells. It is important to emphasize that both uterine horns were clearly enlarged in the estrogen-treated animals in comparison with the non-treated pre-pubertal rats. This effect confirms that the estrogen levels (exogenously administered) are able to induce a physiological response in an estrogen-dependent tissue of pre-pubertal female rats. There is evidence that accentuated levels of a determined hormone promote hormonal cell sensibility due to an increased number of receptors (Rhoades & Tanner, 1995). In the prostate of newborn male rats, treatment with diethylstilbestrol induces an accentuated expression of estrogen receptors (Khurana et al. 2000). Thus, the changes induced by estrogen in the alveolar bone osteoclasts may be related to a physiological response. This is reinforced by the fact that similar morphological changes in osteoclasts were also observed under physiological conditions. In the osteoclasts of female rats during the peak of estrogen, immediately following lactation, the high estrogen levels coincided with the disappearance of osteoclast-ruffled borders, retraction of the osteoclasts from the bone surface, cellular fragmentation and apoptosis (Miller &

Bowman, 2007). However, further studies focusing on a comparative analysis between the results of this study and physiological conditions (i.e. adult female rats in estrus) would be useful.

There is evidence that osteoclast size is also directly associated with its resorptive activity (Lees & Heersche, 2000; Lees et al. 2001). The bone surface in close juxtaposition to osteoclast has been used to estimate the osteoclast activity (Chow et al. 1992). Our findings revealed that the significant reduction in the osteoclast area was accompanied by a reduction in bone resorption surface. Our results indicate, therefore, that the resorptive activity of alveolar bone osteoclasts decreases in estrogen-treated rats.

Enzymatic activities have also been used as indicators of the resorptive activity of osteoclasts (Parikka et al. 2001). It has been shown that weak MMP-9 and cathepsin K immunolabelling in small osteoclasts reflects a reduced capacity for bone degradation (Hu et al. 2008). Although estrogen induces osteoclast apoptosis, differences in the frequency of MMP-9-positive osteoclasts and in the intensity of MMP-9 immunoexpression were not observed. Moreover, the combined MMP-9/TUNEL reactions revealed that apoptotic osteoclasts were positive to MMP-9-immunolabelling.

Therefore, the reduction of the resorptive activity of osteoclasts may not be due to an interference of estrogen treatment on the MMP-9 immunoexpression. It is important to emphasize that apoptotic osteoclasts lose the clear zone and ruffled border (Ito et al. 1999, 2001; Faloni et al. 2007; Cruzoé-Souza et al. 2009). Moreover, estrogen interferes with osteoclast attachment to its substrate (Liu et al. 2002; Saintier et al. 2006), and, thereby, affect the depth of resorption pits (Parikka et al. 2001). Considering that the frequency of MMP-9-positive osteoclasts was not affected by estrogen, the reduction in the bone resorption may be due to an interference of estrogen with the releasing process of this enzyme by the dying osteoclasts. This idea is reinforced by the alterations observed in the vimentin filaments; these filaments are associated with the attachment of the osteoclast to the bone surface which is essential to osteoclast polarization, activation and capacity to degrade bone (Ross & Teitelbaum, 2005; Teitelbaum, 2006). In a study using culture of a mixed rat bone cell population, it was observed that estrogen interferes with the enzymatic degradation of collagen by cathepsin K, but not in the osteoclast MMP-9 activity (Parikka et al. 2001).

In conclusion, our results indicate that estrogen induces alterations in the structural integrity of the osteoclasts from alveolar bone. Thus, the significant decrease/reduction in bone resorption is probably due to a reduction in the number of nuclei and area of osteoclasts rather than to an interference of estradiol with the osteoclast MMP-9 expression. The apoptotic process in osteoclasts includes caspase-3 activity and vimentin degradation, leading to disruption and collapse of the osteoclast cytoplasm, loss of the ruffled border and sealing zone, as well as cytoplasm shrinking. The mononucleated portions derived from the apoptotic osteoclast undergo fragmentation, probably giving rise to TRAP-positive apoptotic bodies, which seem to be engulfed by neighbouring cells.

Acknowledgements

The authors wish to thank Mr. Luis Antônio Potenza and Mr. Pedro Sérgio Simões for technical support. This research was supported by CAPES, CNPq, FUNDUNESP and FAPESP (04/09898-0) – Brazil.

References

Akisaka T, Yoshida H, Suzuki R, et al. (2008) Adhesion structures and their cytoskeleton-membrane interactions at podosomes of osteoclasts in culture. *Cell Tissue Res* **331**, 625–641.

Alam MS, Ohsako S, Tay TW, et al. (2010) Di(n-butyl) phthalate induces vimentin filaments disruption in rat sertoli cells: a possible relation with spermatogenic cell apoptosis. *Anat Histol Embryol* **39**, 186–193.

Bord S, Ireland DC, Beavan SR, et al. (2003) The effects of estrogen on osteoprotegerin, RANKL, and estrogen receptor expression in human osteoblasts. *Bone* **32**, 136–141.

Byun Y, Chen F, Chang R, et al. (2001) Caspase cleavage of vimentin disrupts intermediate filaments and promotes apoptosis. *Cell Death Differ* **8**, 443–450.

Cerri PS (2005) Osteoblasts engulf apoptotic bodies during alveolar bone formation in the rat maxilla. *Anat Rec* **286**, 833–840.

Cerri PS, Freymüller E, Katchburian E (2000) Apoptosis in the early developing periodontium of rat molars. *Anat Rec* **258**, 136–144.

Cerri PS, Boabaid F, Katchburian E (2003) Combined TUNEL and TRAP methods suggest that apoptotic bone cells are inside vacuoles of alveolar bone osteoclasts in young rats. *J Periodont Res* **38**, 223–226.

Cerri PS, Pereira-Júnior JA, Barrionuevo NB, et al. (2010) Mast cells and MMP-9 in the lamina propria during eruption of rat molars: quantitative and immunohistochemical evaluation. *J Anat* **217**, 116–125.

Chow JWM, Lean JM, Chambers TJ (1992) 17β-estradiol stimulates cancellous bone formation in female rats. *Endocrinology* **130**, 3025–3032.

Cruzoé-Souza M, Sasso-Cerri E, Cerri PS (2009) Immunohistochemical detection of estrogen receptor β in alveolar bone cells of estradiol-treated female rats: possible direct action of estrogen on osteoclast life span. *J Anat* **215**, 673–681.

Faloni APS, Sasso-Cerri E, Katchburian E, et al. (2007) Decrease in the number and apoptosis of alveolar bone osteoclasts in estrogen-treated rats. *J Periodont Res* **42**, 193–201.

Gavrieli Y, Sherman Y, Ben-Sasson SA (1992) Identification of programmed cell death *in situ* via specific labeling of nuclear DNA fragmentation. *J Cell Biol* **119**, 493–501.

Hu Y, Ek-Rylander B, Karlström E, et al. (2008) Osteoclast size heterogeneity in rat long bones is associated with differences in adhesive ligand specificity. *Exp Cell Res* **314**, 638–650.

Huppertz B, Frank HG, Kaufmann P (1999) The apoptosis cascade – morphological and immunohistochemical methods for its visualization. *Anat Embryol (Berl)* **200**, 1–18.

Ito M, Amizuka N, Nakajima T, et al. (1999) Ultrastructural and cytochemical studies on cell death of osteoclasts induced by bisphosphonate treatment. *Bone* **25**, 447–452.

Ito M, Amizuka N, Nakajima T, et al. (2001) Bisphosphonate acts on osteoclasts independent of ruffled borders in osteoclerotic (oc/oc) mice. *Bone* **28**, 609–616.

Kanzaki H, Chiba M, Arai K, et al. (2006) Local RANKL gene transfer to the periodontal tissue accelerates orthodontic tooth movement. *Gene Ther* **13**, 678–685.

Kawamoto S, Ejiri S, Nagaoka E, et al. (2002) Effects of estrogen deficiency on osteoclastogenesis in the rat periodontium. *Arch Oral Biol* **47**, 67–73.

Khurana S, Ranmal S, Ben-Jonathan N (2000) Exposure of newborn male and female rats to environmental estrogens: delayed and sustained hyperprolactinemia and alterations in estrogen receptor expression. *Endocrinology* **141**, 4512–4517.

Lee JC, Schickling O, Stegh AH, et al. (2002) DEDD regulates degradation of intermediate filaments during apoptosis. *J Cell Biol* **158**, 1051–1066.

Lees RL, Heersche JN (2000) Differences in regulation of pH_i in large (≥10 nuclei) and small (≤5 nuclei) osteoclasts. *Am J Physiol Cell Physiol* **279**, C751–C761.

Lees RL, Sabharwal VK, Heersche JN (2001) Resorptive sate and cell size influence intracellular pH regulation in rabbit osteoclasts cultured on collagen-hydroxyapatite films. *Bone* **28**, 187–194.

Liu CC, Howard GA (1991) Bone-cell changes in estrogen-induced bone-mass, increase in mice: dissociation of osteoclasts from bone surfaces. *Anat Rec* **229**, 240–250.

Liu BY, Wu PW, Bringhurst FR, et al. (2002) Estrogen inhibition of PTH-stimulated osteoclast formation and attachment *in vitro*: involvement of both PKA and PKC. *Endocrinology* **143**, 627–635.

Miller SC, Bowman BM (2007) Rapid inactivation and apoptosis of osteoclasts in the maternal skeleton during the bone remodeling reversal at the end of lactation. *Anat Rec* **290**, 65–73.

Minkin C (1982) Bone acid phosphatase: tartrate-resistant acid phosphatase as a marker of osteoclast function. *Calcif Tissue Int* **34**, 285–290.

Parikka V, Lehenkari P, Sassi ML, et al. (2001) Estrogen reduces the depth of resorption pits by disturbing the organic bone matrix degradation activity of mature osteoclasts. *Endocrinology* **142**, 5371–5378.

Phan TCA, Xu J, Zheng MH (2004) Interaction between osteoblast and osteoclast: impact in bone disease. *Histol Histopathol* **19**, 1325–1344.

Rhoades RA, Tanner GA (1995) *Medical Physiology*. Boston: Little, Brown and Company.

Rogers A, Saleh G, Hannon RA, et al. (2002) Circulating estradiol and osteoprotegerin as determinants of bone turnover and bone density in postmenopausal women. *J Clin Endocrinol Metab* **87**, 4470–4475.

Ross FP, Teitelbaum SL (2005) Alphavbeta3 and macrophage colony-stimulating factor: partners in osteoclast biology. *Immunol Rev* **208**, 88–105.

Saintier D, Khanine V, Uzan B, et al. (2006) Estradiol inhibits adhesion and promotes apoptosis in murine osteoclasts *in vitro*. *J Steroid Biochem Mol Biol* **99**, 165–173.

Sasso-Cerri E, Freymüller E, Miraglia SM (2005) Testosterone-immunopositive primordial germ cells in the testis of the bullfrog, *Rana catesbeiana*. *J Anat* **206**, 519–523.

Silberberg M, Silberberg R (1941) Further investigations concerning the influence of estrogen on skeletal tissues. *Am J Anat* **69**, 295–331.

Sorensen MG, Henriksen K, Schaller S, et al. (2007) Characterization of osteoclasts derived from $CD14^+$ monocytes isolated from peripheral blood. *J Bone Miner Metab* **25**, 36–45.

Sternlicht MD, Werb Z (2001) How matrix metalloproteinases regulate cell behavior. *Annu Rev Cell Dev Biol* **17**, 463–516.

Tapp E (1966) The effects of hormones on bone in growing rats. *J Bone Joint Surg Br* **48**, 526–531.

Teitelbaum SL (2006) Osteoclasts and integrins. *Ann N Y Acad Sci* **1068**, 95–99.